Photoinitiation and Monomer Segregation Behavior in Polymerization of Lyotropic Liquid Crystalline Systems

Michael A. DePierro and C. Allan Guymon*

Department of Chemical and Biochemical Engineering, University of Iowa, Iowa City, Iowa 52242-1527

Received August 17, 2005; Revised Manuscript Received October 17, 2005

ABSTRACT: Lyotropic liquid crystals (LLC's) have recently been employed as polymerization templates to yield highly ordered nanostructured materials with potential applications in regulated transport, ultrafiltration, and catalysis. With the goal of understanding the reaction mechanisms ultimately determining polymer morphology in these highly ordered systems, this study focuses on the influence of LLC order on photoinitiation efficiency and monomer segregation behavior. These phenomena have been elucidated through extensive examination of the polymerization kinetics utilizing photodifferential scanning calorimetry. The polymerization kinetics in these ordered liquids are highly dependent on phase morphology because liquid crystalline alignment has a profound effect on monomer segregation, and photoinitiation efficiency is a function of viscosity, polarity, and the diffusional constraints inherent in LLC phases. Through studies of the polymerization kinetics in different LLC phases using a free radical inhibitor, the relative initiation efficiencies of a number of photoinitiators were determined. By incorporating relative efficiency information in the analysis of propagation and termination rate parameters, the individual contributions of monomer segregation and photoinitiation behavior to the polymerization kinetics were differentiated. While segregation of polar monomers in the continuous phase leads to increased polymerization rate in more ordered LLC phases, nonpolar monomers exhibit the opposite trend due to segregation in the discontinuous region of the phases studied. Changes in photoinitiation efficiency either compound or negate the effect of monomer segregation on the polymerization rate depending on initiator structure and polarity. The initiation efficiency with relatively bulky, hydrophobic initiators increases substantially in more ordered systems while the efficiency of less hydrophobic initiators decreases slightly in more ordered phases.

Introduction

Many of the techniques used to synthesize materials with nanoscale architectural control rely on self-assembly of molecules into ordered arrays possessing nanoscopic dimensions.[1] One particularly versatile method offering great promise in the controllable synthesis of nanostructured polymeric materials involves self-assembly of amphiphillic molecules into highly ordered lyotropic liquid crystalline (LLC) arrays. These interesting materials exhibit low viscosities characteristic of fluids while maintaining highly complex and periodic morphology more typical of crystalline materials.[2] As the concentration of surfactant is varied in a typically polar solvent, a variety of LLC structures may be observed ranging from highly curved micellar and discontinuous cubic aggregates, which form at low concentrations of amphiphile, to rodlike arrangements of micelles in the hexagonal phase. The lamellar phase, exhibiting minimal curvature, as well as inverted structures of the previously mentioned phases may form at higher surfactant concentrations depending on the nature of the surfactant and solvent.[3]

While a lack of mechanical strength and thermal stability has previously limited the use of lyotropic liquid crystals in materials applications, more robust materials possessing LLC morphology have recently been obtained using various amphiphillic, cross-linking monomers.[4−7] The novel properties of the resulting polymers have shown promise in advancing diverse applications such as size exclusion barriers,[8] catalysts,[9,10] and nanocomposites.[11] Through careful synthetic design of cross-linking monomers, feature size can be controlled to provide the necessary properties for a variety of applications.[12] Several LLC phases have also recently been templated through a similar approach using conventional monomers with full retention of original order in cross-linked networks.[13−17] By taking advantage of the wide range of known phase behaviors in different LLC systems, this method could enable facile control of polymer structure by preselecting a template phase with the desired geometry.[18−21]

Initial investigations of the polymerization kinetics in templated LLC systems have revealed that the polymerization kinetics play a critical role in ultimate polymer structure and properties. Better retention of LLC order has been linked to higher polymerization rates, and loss of LLC morphology from phase separation appears more prevalent at lower rates of polymerization.[6,7,14] The diffusional limitations inherent to liquid crystals cause unique polymerization kinetics not observed in bulk or solution polymerization.[22−26] Polymerization of acrylamide, which proceeds quite slowly in isotropic solution, occurs much more rapidly in highly organized cubic and hexagonal phases as the monomer aligns topologically along the surfactant/water interface.[14,15] Monomer polarity plays a unique role in the kinetics in LLC systems as polar and nonpolar monomers segregate to different regions of LLC phases. While polar monomers, such as acrylamide and poly(ethylene glycol) dimethacrylate, become increasingly ordered and polymerize faster in more ordered LLC systems, nonpolar monomers, such as hexanediol diacrylate and *n*-decyl acrylate, polymerize more slowly as LLC order increases as a result of decreased localized double bond concentration.[13,27]

Just as segregation of monomers of different polarity causes distinct polymerization behavior, the chemical structure of the initiator may likewise dictate how initiators localize in LLC systems, thereby impacting the polymerization kinetics and ultimate polymer structure. Several studies using emulsion

* To whom all correspondence is to be addressed: e-mail allan-guymon@uiowa.edu; Ph (319)-335-5015; Fax (319)-335-6086.

10.1021/ma0518196 CCC: $33.50
Published on Web 12/17/2005

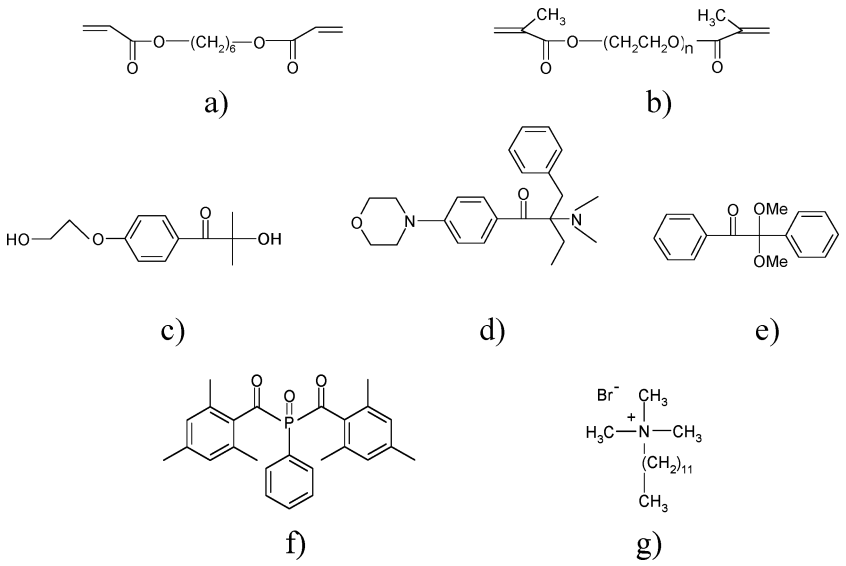

Figure 1. Chemical structures of the monomers, photoinitiators, and surfactant used in this study. Shown are (a) hexanediol diacrylate (HDDA), (b) poly(ethylene glycol)-400 dimethacrylate (PEGDMA), (c) 2-hydroxy-1-[4-(2-hydroxyethoxy)phenyl]-2-methyl-1-propanone (HEPK), (d) 2-benzyl-2-(dimethylamino)-1-[4-(4-morpholinyl)phenyl]-1-butanone (DBMP), (e) α,α-dimethoxy-α-phenylacetophenone (DMPA), (f) bis(2,4,6-trimethylbenzoyl)phenylphosphine oxide (BAPO), and (g) dodecyltrimethylammonium bromide (DTAB).

polymerization have shown distinctly different kinetics and polymer molecular weight evolution when using photoinitiators of different polarity.[28−31] Studies of photochemical reactions in micelles,[32,33] vesicles,[34] and thermotropic liquid crystals[35,36] have demonstrated a strong relationship between radical formation and decay on solvent order. For example, in thermotropic liquid crystals photodecomposition of alkylphenones results in higher degrees of cyclic product formation in isotropic solution relative to that in the smectic phase due to a less rigid and less structured environment.[35] The occurrence of in-cage recombination of radical pairs from photolysis of dibenzyl ketones is also dependent on the phase type of the reaction environment as well as local viscosity.[36] Such recombination reactions could significantly impact photopolymerization in ordered LLC systems by lowering the rate of initiation and overall rate of polymerization.

Initiator structure will play a unique role in the polymerization behavior in LLC media because of the confined geometry and polarity considerations in the highly ordered surfactant phases. The goal of this study is to elucidate the relationship between photoinitiator structure and polymerization kinetics in LLC systems. The influence of LLC order on initiation efficiency and monomer segregation will be studied to gain a more complete understanding of the complex dynamics governing polymer structure. The rate of polymerization of two cross-linking monomers will be compared using several common photoinitiators of different polarity and mobility in various LLC phases. Individual contributions of monomer and photoinitiator effects to the polymerization behavior will be evaluated by comparing rate constants of propagation and termination under various reaction conditions and incorporating relative initiation efficiency information obtained with a free radical inhibitor. Since initiator efficiency is directly related to the molecular weight in linear polymer systems, further understanding of initiation efficiency will be obtained by studying the polymer molecular weight evolution as a function of both LLC phase and initiator structure. A better understanding of the role of photoinitiator in these morphologically complex reaction systems could enable the future design and selection of initiators for better structural control.

Experimental Section

Materials. The photoinitiators compared in the study were 2-hydroxy-1-[4-(2-hydroxyethoxy)phenyl]-2-methyl-1-propanone (HEPK, Ciba Specialty Chemicals), 2-benzyl-2-(dimethylamino)-1-[4-(4-morpholinyl)phenyl]-1-butanone (DBMP, Ciba Specialty Chemicals), bis(2,4,6-trimethylbenzoyl)phenylphosphine oxide (BAPO, Ciba Specialty Chemicals), and α,α-dimethoxy-α-phenylacetophenone (DMPA, Ciba Specialty Chemicals). The polymerization kinetics with each initiator were compared using the hydrophobic hexanediol diacrylate (HDDA, Polysciences) and the water-soluble poly(ethylene glycol)-400 dimethacrylate (PEGDMA, Polysciences). Molecular weight was determined of polymers synthesized with *n*-decyl acrylate (Polysciences). This monomer was chosen for the study because it exhibits similar kinetic behavior to HDDA while forming linear polymer. Hydroquinone (Aldrich) was utilized to inhibit polymerization in the comparison of initiation efficiency. Liquid crystalline samples were synthesized using varying concentrations of the cationic surfactant dodecyltrimethylammonium bromide (DTAB, Aldrich) and deionized water. Samples were mixed, centrifuged, and sonicated repeatedly until homogeneous gels were obtained. Figure 1 shows the chemical structures of the materials used in this study.

Methods. Lyotropic liquid crystal morphology and phase boundaries were characterized with a polarized light microscope (Nikon, Eclipse E600W Pol) equipped with a hot stage (Instec, Boulder, CO) by examining the optical texture of each sample. For corroboration of microscopy data, phase identities were identified with small-angle X-ray scattering by measuring ratios in *d* spacing. These measurements were conducted utilizing a Nonius FR590 X-ray apparatus with a standard copper target Röntgen tube as the radiation source with a Cu Kα line of 1.54 Å, a collimation system of the Kratky type, and a PSD 50M position sensitive linear detector (Hecus M. Braun, Graz).

Polymerization rate data were acquired with a Perkin-Elmer differential scanning calorimeter. The emission spectrum from a medium-pressure UV arc lamp (Ace Glass) was used to initiate polymerizations. Light intensity was controlled with optical filters and by varying the distance of the sample from the lamp. For the majority of the kinetics experiments full spectrum, 60 mW/cm^2 light was used. However, the experiments to determine kinetic constants were conducted with 365 nm light with intensity of 1.6 mW/cm^2. Error caused by water evaporation was minimized by covering the ∼5 mg samples with thin transparent films of FEP (Dupont fluorinated copolymer). Samples were purged with nitrogen for 6

min prior to polymerization to prevent oxygen inhibition. Isothermal reaction conditions were maintained during polymerization using a refrigerated circulating chiller. The polymerization rate, R_p, was determined as a function of time from the heat flow (Q) according to eq 1

$$R_p = \frac{Q[M_0]MW}{\Delta HM} \quad (1)$$

where $[M_0]$ is the initial monomer concentration, MW is the monomer molecular weight, ΔH is the enthalpy of polymerization of the monomer, and M is the sample mass. Maximum rates were taken from the peak in the rate profiles obtained, and double-bond conversion was calculated by integrating the heat flow profiles.[25] For these studies the theoretical values of 20.6 and 13.1 kcal/mol were used as the heat evolved per reacted acrylate and methacrylate double bond, respectively.[37] The relative standard error for these kinetic experiments was calculated by dividing the standard deviation of the maximum polymerization rate from five identical experiments by the average. While the error varied significantly from sample to sample, the relative standard error for the vast majority of samples was less than 10%. Apparent rate parameters for k_t and k_p were measured through a series of after-effect experiments. The steady-state polymerization rate was utilized to determine the lumped kinetic constant, $k_p/k_t^{1/2}$ as a function of time. By closing the light shutter at various time intervals during the polymerization, the initiation step was eliminated and the exotherm decay was analyzed according to eq 2

$$\frac{1}{R_p} - \frac{1}{R_{p0}} = \frac{2k_t t}{k_p[M]} \quad (2)$$

where R_p is the polymerization rate at time t, R_{p0} is the initial rate of polymerization, and [M] is the monomer concentration at time t. The term $2k_t t/k_p[M]$, obtained from plotting $1/R_p$ with respect to time of the dark reaction, was combined with the lumped kinetic constant from the steady-state reaction to decouple apparent propagation and termination kinetic parameters. This method of determining individual rate parameters is described in detail elsewhere.[25]

A gel permeation chromatography system with a PLgel Mixed D 300 × 7.5 mm column from Polymer Labs was used to characterize polymer molecular weight. The Shimadzu instrumental setup included a differential refractomeric detector, RID-10A, a solvent delivery pump, LC-10ATVP, and a system controller SCL-10AVP. Polymer samples with concentration of ~1.0 mg/cm^3 were eluted at 1 cm^3/min in tetrahydrofuran (THF). A universal calibration curve was constructed using eight narrow range polystyrene standards with molecular weights ranging from 4×10^3 to 1×10^6 g/mol.

Results and Discussion

The polymerization kinetics in lyotropic liquid crystalline media are highly dependent on the degree of order in the reaction medium. Changes in polymerization rate observed in differently ordered LLC systems have been attributed to monomer segregation and ordering phenomena. For example, nonpolar monomers become highly locally concentrated in the lypophillic domains of the cubic phase and consequently polymerize more rapidly than in the hexagonal and lamellar phase, where localized double bond concentrations are lower.[13,27] Polar monomers exhibit significantly different behavior, with more rapid polymerization observed in lamellar and hexagonal phases due to higher degrees of monomer ordering.[14,15] The interaction of photoinitiator with the surfactant aggregates could similarly impact the polymerization kinetics. Since medium polarity, viscosity, and order are known to affect the photochemical reactions of a number of compounds,[28,33−36,38,39] the formation of free radical pairs from initiator photolysis may therefore be highly dependent on LLC morphology.

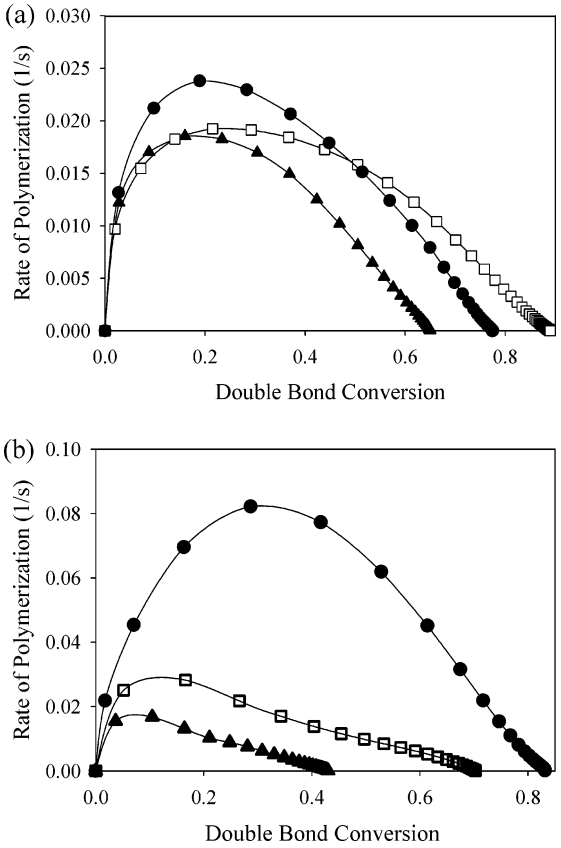

Figure 2. Polymerization profiles of 20% PEGDMA initiated with (a) 0.2 wt % HEPK and (b) 0.2 wt % DBMP. Shown are polymerizations in 40% discontinuous cubic (▲), 60% hexagonal (□), and 70% lamellar (●) DTAB in water.

It is well known that different photoinitiators, due to varying absorbance characteristics, yield different rates of polymerization in isotropic bulk polymerizations. In LLC systems local variations in morphology, viscosity, and composition introduce more complex photoinitiation dynamics. To understand how these factors may influence the polymerization in LLC systems, the polymerization rate with respect to LLC order has been compared using several common α-cleavage photoinitiators. A wide variety of liquid crystalline phases, ranging from discontinuous cubic, hexagonal, to lamellar form as the concentration of DTAB, a cationic surfactant, is varied in water, making it an ideal system for the study. To demonstrate the effect of liquid crystalline order on the polymerization kinetics, Figure 2 shows polymerization profiles of PEGDMA with two initiators in the phases that form as DTAB concentration is varied in water. For polymerizations initiated with the relatively water-soluble HEPK, as shown in Figure 2a, the polymerization rate is lowest in the discontinuous cubic phase. In the hexagonal phase, at higher concentrations of surfactant, the rate and conversion both increase. When the surfactant concentration is increased to 70 wt %, the degree of order in the system further increases to form the lamellar phase in which the highest polymerization rate is observed. By simply changing the order of the liquid crystalline system, a 40% increase in rate occurs in polymerizations initiated with HEPK. Similar rate enhancements observed in continuous phase polymerization have previously been attributed to an increase in monomer ordering from association of the polar monomer with surfactant aggregates.[13,27]

To understand whether changes in photoinitiation behavior may also contribute to the enhanced rate observed in the more

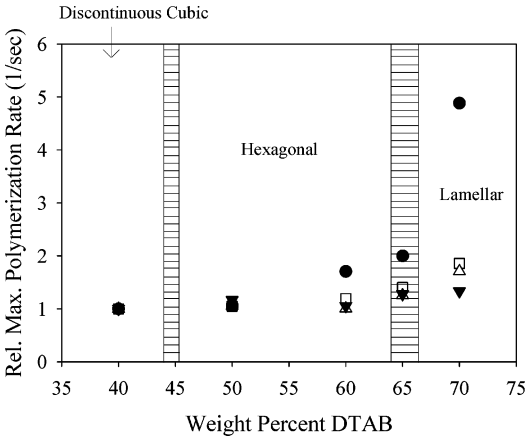

Figure 3. Relative maximum rate of polymerization of 20% PEGDMA initiated with 0.2 wt % HEPK (▼), DMPA (△), BAPO (□), and DBMP (●) in the LLC phases of DTAB/water with respect to DTAB concentration.

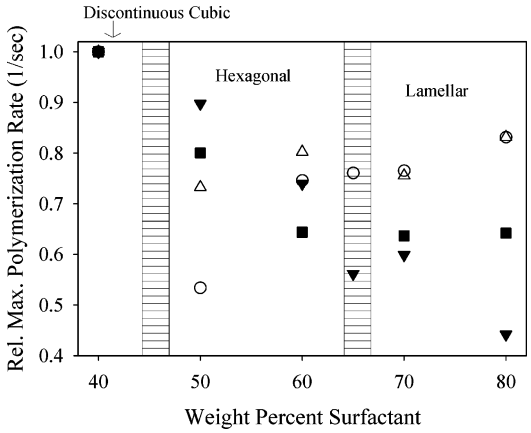

Figure 4. Relative peak polymerization rate of 10% HDDA initiated with 0.1 wt % HEPK (▼), DMPA (■), DBMP (○), and BAPO (△) in the LLC phases of DTAB/water as a function of DTAB concentration.

ordered LLC phases, the polymerization rate was also monitored in the same liquid crystalline system with the more bulky, relatively hydrophobic photoinitiator, DBMP. As shown in Figure 2b, the general trend of increasing rate with increasing LLC order is also observed with this initiator, although the magnitude of increase in this case is much greater. Again, polymerization is slowest in the discontinuous cubic phase, but with this initiator the rate nearly doubles in the hexagonal phase. The most remarkable difference with DBMP is the dramatic rate increase observed in the lamellar phase. In contrast to HEPK, for which the rate increases by half between the discontinuous cubic and lamellar phases, more than a 4-fold rise in rate occurs with the hydrophobic DBMP. From these results it is apparent that distinct photoinitiation behavior, not just monomer segregation, contributes to the changes in polymerization rate in different phases.

To gain a broader understanding of the effect of photoinitiator on polymerization in ordered surfactant systems, the polymerization kinetics were similarly examined using two other common α-cleavage initiators, DMPA and BAPO. Initiators used in the study were selected in order to provide understanding of the effect of radical size and polarity on the polymerization kinetics. Figure 3 shows the maximum rate of polymerization with these initiators in addition to HEPK and DBMP. As mentioned previously, polymerization with PEGDMA in the LLC phases of the DTAB/water system in general exhibits the trend of increasing rate with increasing LLC order. However, the influence of the photoinitiator manifests itself by the magnitude of increase observed with each initiator as the composition and order of the reaction environment are changed. The smallest dependence of polymerization rate on LLC order is observed with the most hydrophilic initiator, HEPK. With DMPA, a less polar initiator of approximately the same molecular weight, the rate increases by almost 70% between the discontinuous cubic and the lamellar phase. The rate of polymerization with BAPO exhibits an even greater dependence on LLC order. The highest dependence of rate on order is observed with the bulky, highly hydrophobic initiator, DMPB, with which the rate increases 400% over the same composition range. With each initiator the greatest increase in rate occurs above 60 wt % surfactant with the transition to lamellar morphology. Although the photoinitiator is added to these systems in concentrations of 1 wt % relative to monomer (0.2 wt % of total sample), changes in photoinitiator structure appear to significantly impact the polymerization behavior.

To determine whether the photoinitiator plays a similar role in the kinetics when monomer is sequestered within the discontinuous phase, the polymerization rate of HDDA with respect to LLC order was similarly examined using initiators of different size and hydrophobicity. Comparing the trend in polymerization rate as a function of LLC order with the same initiators used to study PEGDMA could indicate whether the effect of initiator on the polymerization rate in LLC systems is similar to monomers of different polarity and aid in differentiating the effects of monomer polarity and photoinitiator characteristics on the polymerization kinetics in these complex systems. The relative maximum rate of polymerization of HDDA with several photoinitiators in the LLC phases of DTAB and water is shown in Figure 4. The absolute rate of polymerization at each concentration of surfactant is divided by the rate in the discontinuous cubic phase at 40 wt % DTAB to allow facile comparison of the trends in rate behavior. As seen with PEGDMA, distinct discontinuous cubic, hexagonal, and lamellar phases are observed with HDDA at varying concentrations of DTAB and water although phase boundaries are slightly shifted. With all of the initiators in the study, the transition from the cubic to the hexagonal phase results in a lower rate of polymerization. However, as surfactant concentration is further increased to induce transition from the hexagonal to a lamellar phase, great differences in this trend are seen with the different initiators. As shown in Figure 4, the rate continually decreases with DMPA and HEPK as surfactant concentration increases, with greater rate decreases in the HEPK systems. With the relatively bulky and hydrophobic BAPO the rate initially decreases with the transition to the hexagonal phase but remains relatively constant with increasing surfactant concentration. With DBMP, which is also very hydrophobic, the trend in polymerization rate with respect to LLC order contrasts markedly with the other initiators. After dropping by half between the cubic and hexagonal phase, the rate nearly doubles at higher concentrations of surfactant with the transition to a lamellar morphology.

To understand the factors driving the change in polymerization rate with each initiator, we first consider the equation commonly used to describe the rate of free radical polymerization, which assumes steady-state conditions and bimolecular termination

$$R_p = k_p[M]\left(\frac{R_i}{2k_t}\right)^{1/2} \quad (3)$$

where [M] is the momonomer concentration, k_p and k_t are rate coefficients of propagation and termination, respectively, and R_i is the rate of initiation.[40] To determine the cause of the distinct polymerization behavior observed with different initiators, primary consideration should be given to the factors influencing R_i, which is given by

$$R_i = 2\phi\epsilon I_0[I] \quad (4)$$

where ϕ is the initiation efficiency, ϵ is the molar extinction coefficient, I_0 is the light intensity, and [I] is the photoinitiator concentration. Differences in extinction coefficients of the different initiators, while highly influential in the absolute rate of polymerization, do not explain the different trends in rate with respect to surfactant concentration. Since the light intensity was not varied within a sample in the kinetic studies, the different trends in polymerization rate are most likely tied to the initiation efficiency, ϕ, defined as the fraction of radicals formed from photolysis, which are successful in initiating polymerization.[41,42] Upon decomposition of initiator, the radicals formed may undergo many types of reactions within the solvent cage including recombination or reactions forming species that cannot initiate polymerization. The lowering of the initiator efficiency by these "in cage" reactions is known as the cage effect and is known to be prevalent in photoinitiated polymerizations.[40] Initiation efficiency is known to depend on a number of factors such as monomer and initiator selection as well as medium viscosity, pH, and polarity.[28,29,42−44] Several studies have also demonstrated a significant dependence of initiation efficiency on solvent ordering.[33,34,36]

Inhibition Experiments. One common method for evaluating photoinitiation efficiency utilizes free radical inhibitors. At sufficient concentrations of inhibitor, where polymerization rate is considerably reduced, bimolecular termination is negligible, and the rate of polymerization becomes dependent on the first power of the initiation rate given by

$$R_p = \frac{k_p[M]R_i}{k_z[Z]} \quad (5)$$

where k_z is the rate constant for inhibition and [Z] is the concentration of inhibitor.[40] Under such conditions, bimolecular termination is negligible, and the overall polymerization rate is directly proportional to the rate of initiation. By monitoring the effect of inhibitor concentration on the polymerization rate, the relative initiation efficiency may be compared in different LLC phases.

To verify the effectiveness of this method, a control experiment was conducted in which the rate of polymerization of neat HDDA was determined with respect to inhibitor concentration using different concentrations of photoinitiator. In Figure 5 the relative maximum rate of polymerization of neat HDDA is plotted with respect to hydroquinone concentration. To allow direct comparison of the effect of inhibitor on the polymerization, the relative decrease in rate of polymerization was determined using three concentrations of the photoinitiator, HEPK. The relative maximum rate at each concentration of inhibitor was calculated by dividing by the maximum polymerization rate determined without inhibitor. In this study the relative maximum rate is consistent with the relative rate at other conversions and can therefore be used to represent the general trend in polymerization rate. With 0.5 wt % HEPK, a 90% decrease in rate occurs upon adding 0.4 wt % hydroquinone. When 1 wt % initiator is used, a similar decrease in rate requires twice as much hydroquinone. While the rate decreases significantly for all initiator concentrations, this experiment confirms that the largest decrease occurs with low concentrations of initiator. This behavior is expected since a larger number of free radicals are formed at higher initiator concentrations, requiring a higher concentration of free radical scavenger to have a similar effect on the polymerization rate.

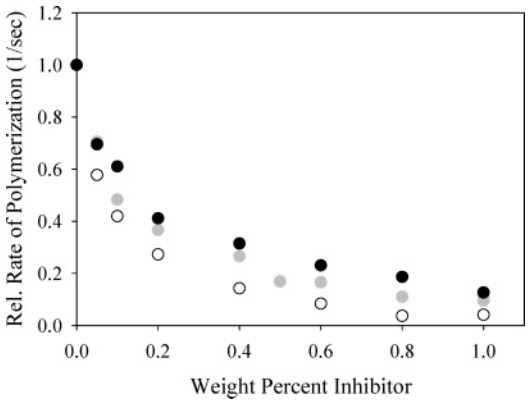

Figure 5. Relative polymerization rate of neat HDDA initiated with 0.5 wt % HEPK (unfilled circles), 1 wt % HEPK (gray circles), and 2 wt % HEPK (black circles) with respect to hydroquinone concentration.

The inhibitor method can be applied to understand how LLC order influences the efficiency of different initiators. Differences in initiation efficiency could explain the distinct trends in polymerization rate observed with the initiators mentioned previously. To determine how LLC order affects the photoinitiation efficiency of the relatively hydrophilic HEPK, the rates of polymerization of PEGDMA in discontinuous cubic, hexagonal, and lamellar phases of DTAB and water were examined with increasing inhibitor concentrations. The relative maximum polymerization rate of PEGDMA initiated with HEPK in each phase is plotted with respect to hydroquinone concentration in Figure 6a. The consistency of data points in the inhibition study shows that efficiency changes are minimal with HEPK. The more rapid decrease in polymerization rate observed in the hexagonal and lamellar phases corresponding to 55 and 70 wt % DTAB indicates that the initiation rate is lowest in these phases. In the discontinuous cubic phase formed with 40 wt % surfactant, higher concentrations of inhibitor are required to reduce the rate, indicating a slightly higher initiation efficiency in this phase with HEPK.

A contrasting trend occurs when polymerization is initiated with DBMP, a more hydrophobic and bulky molecule. In this case the data points are much more widely spaced as shown in Figure 6b, indicating a substantial increase in efficiency between the cubic and lamellar phase. Initiation efficiency is lowest with this hydrophobic initiator in the discontinuous cubic and hexagonal phases evidenced by the 70% drop in rate at 3 wt % hydroquinone. The relatively small decrease in rate in the lamellar phase is indicative of much higher initiation efficiency. Clearly photoinitiation efficiency is dependent on LLC composition and corresponding morphology, and different photoinitiators may exhibit a very distinct dependence on this order.

To understand whether similar changes in initiation efficiency occur with HDDA, the relative effect of inhibitor on the polymerization rate of this monomer in different LLC phases was also studied using DBMP and HEPK. The relative maximum rate of polymerization is plotted with respect to hydroquinone concentration in discontinuous cubic, hexagonal, and lamellar phases using these two initiators in Figure 7. For polymerization initiated with HEPK, as shown in Figure 7a, the rate drops most quickly in the lamellar phase with increasing

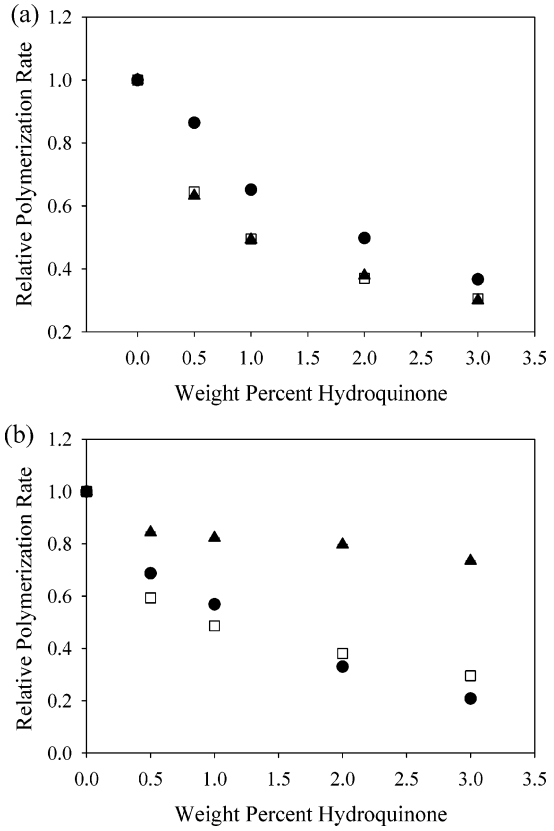

Figure 6. Relative polymerization rate of 20% PEGDMA initiated with (a) 0.2 wt % HEPK and (b) 0.2 wt % DBMP in different LLC phases plotted as a function of hydroquinone concentration. Shown are polymerizations in 40% discontinuous cubic (●), 55% hexagonal (□), and 70% lamellar (▲) DTAB in water.

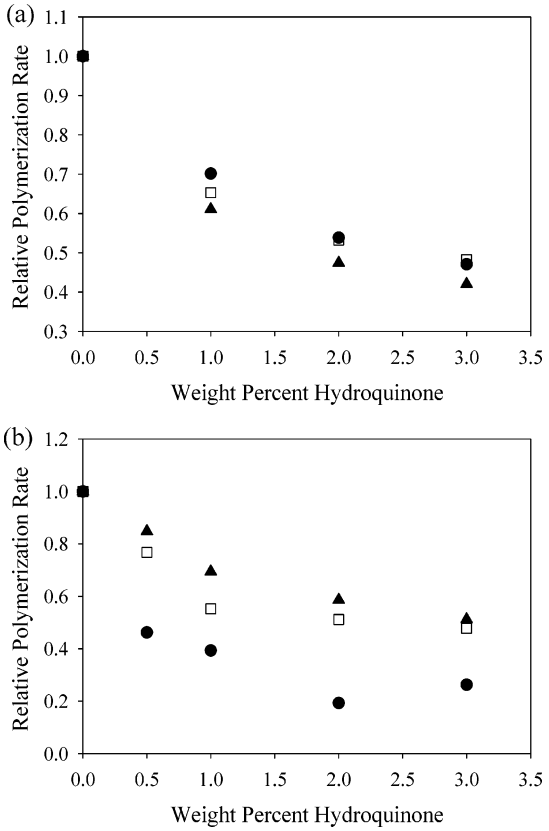

Figure 7. Relative polymerization rate of 10% HDDA initiated with (a) 0.1 wt % HEPK and (b) 0.1 wt % DBMP in different LLC phases plotted as a function of hydroquinone concentration. Shown are polymerizations in 40% discontinuous cubic (●), 55% hexagonal (□), and 70% lamellar (▲) DTAB in water.

inhibitor and least in the cubic phase, with intermediate behavior exhibited in the hexagonal phase. These results are consistent with those from the PEGDMA study, providing further evidence that initiation efficiency with HEPK decreases at higher concentrations of surfactant. It should be noted that this decrease in efficiency is very small, and relative to DPMP the efficiency of HEPK appears nearly independent of LLC order.

As shown in Figure 7b, the initiation efficiency with DBMP changes much more rapidly as LLC composition and morphology are varied. The efficiency with this hydrophobic initiator is highest in the lamellar phase and decreases considerably in the more water-rich hexagonal and cubic phases. The relative efficiency of DBMP in the polymerization of HDDA is similar to that measured with PEGDMA, confirming that changes in LLC morphology are the probable cause of the significant change in initiation efficiency. When this hydrophobic initiator is dispersed within the highly curved lypophillic cores of the discontinuous cubic and hexagonal phase, the escape rate of radicals formed upon photolysis may be rather low, resulting in a low number of radicals available to initiate polymerization. The larger size scale of the hydrophobic domains in the lamellar phase provides a less restricted environment for the relatively immobile, hydrophobic initiator fragments, allowing a greater escape rate of radicals from the solvent cage and a significantly higher initiating radical concentration. As a result, initiation and polymerization occur more rapidly in the lamellar phase with DBMP. The smaller, more mobile, and more hydrophilic radicals formed from the photolytic decomposition of HEPK are less hindered by the cubic and hexagonal structures, and initiation efficiency is therefore not significantly different in the lamellar phase.

After-Effects Experiments. To gain a more complete understanding of all the factors controlling the rate in these systems and to obtain quantitative information about the initiation efficiency in different LLC phases, after-effects experiments were performed to determine apparent rate parameters of propagation, k_p, and termination, k_t. The apparent rate parameters for the polymerization of PEGDMA initiated with HEPK in the 40 and 70 wt % DTAB compositions, corresponding to discontinuous cubic and lamellar morphology, are plotted with respect to double bond conversion in Figure 8. In this experiment apparent k_p and k_t values were calculated from the steady-state polymerization rate and dark reaction exotherm decay using an initiation efficiency, Φ, of 0.6 in both cubic and lamellar phases.[41] Using the same values is consistent with the relatively similar initiation efficiency observed with HEPK in these phases from the inhibition experiments. While apparent k_p values in the cubic and lamellar phases are quite similar, apparent termination rate constants are significantly lower in the lamellar system. This large decrease in the magnitude of the apparent termination rate constant is responsible for the increased rate observed in the lamellar phase. Such a decrease in k_t has similarly been attributed to a significant rate increase in thermotropic LC phases.[23] As other studies have shown that poly(ethylene glycol) aggregates readily with cationic surfactants, this lowering of the apparent k_t could result not only from increased medium viscosity during polymerization but also from close association of the polar monomer with surfactant at the interface.[45]

Since a change in photoinitiator, a component with very low concentration in these samples, would have a negligible effect on monomer organization and LLC order, it should be expected

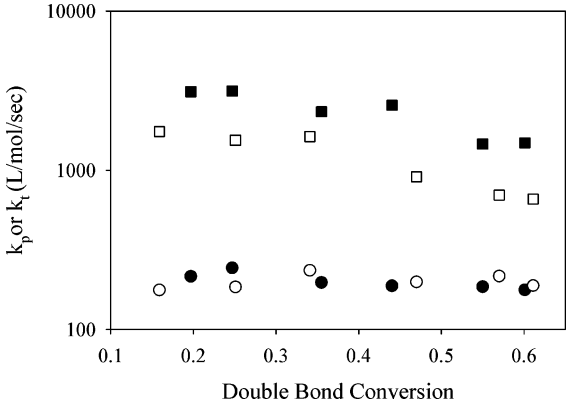

Figure 8. Apparent termination (k_t) and propagation (k_p) rate parameters of 20% PEGDMA initiated with 0.2 wt % HEPK in LLC phases of DTAB/water, shown as a function of double bond conversion. Given are k_t for 70% DTAB-lamellar (□), k_t for 40% DTAB-cubic (■), k_p for 70% DTAB-lamellar (○), and k_p for 40% DTAB-cubic (●). These rate parameters were calculated with $\Phi = 0.6$ in both cubic and lamellar phases.

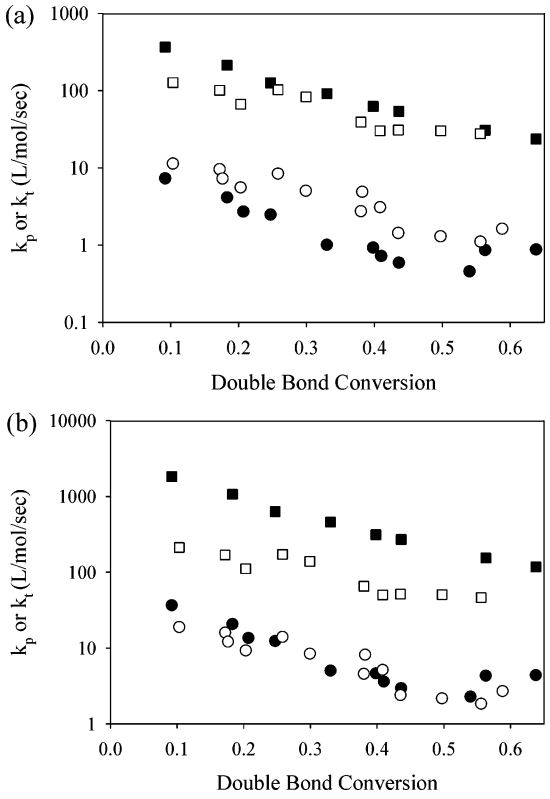

Figure 9. Apparent termination (k_t) and propagation (k_p) rate parameters of 20% PEGDMA initiated with 0.2 wt % DBMP in LLC phases of DTAB/water, shown as a function of double bond conversion. Given are k_t for 70% DTAB-lamellar (□), k_t for 40% DTAB-cubic (■), k_p for 70% DTAB-lamellar (○), and k_p for 40% DTAB-cubic (●). In (a) $\Phi = 0.6$ in both cubic and lamellar phases. Plot (b) accounts for changes in photoinitiation efficiency with $\Phi = 0.2$ in the cubic phase and $\Phi = 0.6$ in the lamellar phase.

that the relative values of apparent k_p and k_t would be similar to that observed with HEPK between the cubic and lamellar phase. In Figure 9 the apparent rate parameters of propagation and termination of PEGDMA initiated with DBMP are plotted with respect to double bond conversion for 40 and 70 wt % DTAB. Figure 9a shows the apparent rate parameters calculated using an initiation efficiency of 0.6 in both cubic and lamellar phases as was done previously with HEPK. If the efficiency is assumed constant in both phases, the resulting trend in apparent k_p and k_t is significantly different than that observed with HEPK. The resulting apparent k_t values in the lamellar sample are slightly lower than those of the cubic sample, while apparent k_p values are up to an order of magnitude higher in the lamellar phase. The change of photoinitiator is unlikely to have such an impact on the trend in apparent k_p and k_t between these samples. The 5-fold increase in the polymerization rate that occurs with DBMP between the cubic and lamellar phase results at least in part from increased initiation efficiency as indicated from the inhibitor experiments in the lamellar phase and not from an apparent increase in k_p only, as these values would indicate.

The inhibition experiments show that initiation efficiency with DBMP changes substantially in the different LLC phases. Potentially erroneous values of apparent k_p and k_t result in this case when changes in efficiency are not considered. To accurately model the polymerization kinetics for initiation with DBMP, the changes in photoinitiation efficiency were accounted for by adjusting the efficiency parameter to match the kinetics data obtained with HEPK, with which there is no change in efficiency from the cubic to the lamellar phase. Accordingly, apparent k_p and k_t values were recalculated using a lower efficiency of 0.2 in the cubic phase and an efficiency of 0.6 in the lamellar phase. The resulting apparent rate constants of propagation and termination are plotted as a function of double bond conversion in Figure 9b. The more accurate inclusion of a lower efficiency in the cubic phase shifts apparent k_p and k_t to higher magnitudes such that the apparent k_t values in the lamellar phase are an order of magnitude lower than that of the cubic phase, and apparent k_p values are of the same magnitude in the cubic and lamellar phase. This decrease in the apparent termination rate parameter from the lamellar phase polymerization is consistent with the results from HEPK and with previous kinetic studies of this system.[13] By using efficiency as an adjustable parameter to model the kinetics, similar kinetic behavior are observed with two different initiating systems. From this model it may be concluded that a decreased apparent rate parameter for termination accounts for the increase in rate observed with both initiators. Significant increase in initiation efficiency also contributes to the more dramatic rate increase observed with DBMP between the cubic and lamellar phase.

After-effects experiments were also performed using HDDA and the same two initiators. Since the initiation efficiency with HEPK changes very little between the cubic, hexagonal, and lamellar phases with HDDA, the trend in apparent k_p and k_t calculated using constant initiation efficiency provides a reasonable representation of the monomer ordering and segregation phenomena governing the rate in this system. If deviations from this trend occur with other initiators, changes in initiation efficiency are the likely cause. This method can thus be used to understand the degree to which changes in monomer organization and segregation and initiation efficiency each influence the polymerization kinetics in these ordered surfactant systems. A plot of the apparent rate parameters of propagation and termination as a function of double bond conversion for HDDA initiated with HEPK in samples containing 50 and 80 wt % DTAB is shown in Figure 10. To calculate apparent k_p and k_t from the DSC experiments, efficiency values of 0.6 were used in both lamellar and hexagonal phases. In going from the rapidly polymerizing hexagonal phase to the lamellar phase, which polymerizes half as fast, apparent k_p and k_t both decrease by an order of magnitude over the full range of conversion. A decrease in apparent k_p alone would cause a decrease in the rate. While a decrease in apparent k_t would actually cause an increase in rate, the overall rate varies proportionally with $k_p/k_t^{1/2}$. Therefore, an equivalent decrease in both apparent k_p and

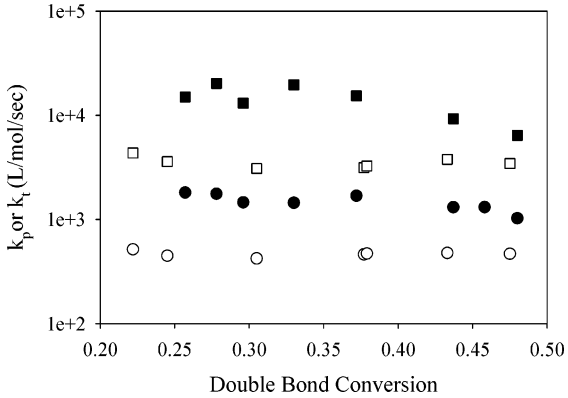

Figure 10. Apparent termination (k_t) and propagation (k_p) rate parameters of 10% HDDA initiated with 0.1 wt % HEPK in LLC phases of DTAB/water, shown as a function of double bond conversion. Given are k_t for 80% DTAB-lamellar (□), k_t for 50% DTAB-hexagonal (■), k_p for 80% DTAB-lamellar (○), and k_p for 50% DTAB-hexagonal (●). These rate parameters were calculated with $\Phi = 0.6$ in both hexagonal and lamellar phases.

k_t would yield an overall decrease in rate. In the hexagonal phase the nonpolar monomer is segregated within the cylindrical aggregates, and high localized double bond concentration causes such elevated apparent k_p and k_t values along with the higher polymerization rate. In the lamellar phase local double bond concentrations are substantially lower as the monomer becomes more diffusely distributed in the system, yielding a lower rate of polymerization.[13,27]

When the α-amino ketone DBMP is used to initiate polymerization of HDDA in the same system, the polymerization rate initially decreases between the cubic and lamellar phase formed at 50 wt % surfactant. Further increases in the surfactant concentration then result in increased rate of polymerization within the hexagonal and lamellar phase. As described with PEGDMA above, the apparent rate constants of propagation and termination were calculated for this system initially using $\phi = 0.6$ in both hexagonal and lamellar phases, as depicted in Figure 11a. In this scenario apparent rate constants of termination are nearly identical over the full range of conversion in the hexagonal and lamellar phase, and the increase in rate appears to result purely from an approximately 5-fold increase in the magnitude of the apparent propagation rate parameter. Not accounting for changes in initiation efficiency between the hexagonal and the lamellar phase likely causes such unusually large increase in the apparent propagation rate parameter. To more accurately model the kinetics with DBMP, the efficiency parameter was again adjusted to match kinetic behavior observed in the HEPK initiating system. The adjusted apparent k_p and k_t values for the polymerization of HDDA initiated with DBMP in the hexagonal and lamellar phases of DTAB/water are plotted as a function of double bond conversion in Figure 11b. Upon adjusting the initiation efficiency to $\phi = 0.06$ in the hexagonal phase and $\phi = 0.6$ in the lamellar phase, the calculated apparent k_p and k_t values are similar to that in the baseline study with HEPK. This type of kinetic analysis, involving comparison of apparent rate constants from different initiators, provides significant information about the factors driving the polymerization kinetics in these systems. The decrease in magnitude of apparent termination and propagation rate parameters in the lamellar phase, which results from a decrease in localized double bond concentration, would expectedly cause a decrease in the polymerization rate. However, this analysis shows that the increase in initiation efficiency, which occurs between the hexagonal and lamellar phase, is a competing effect, which

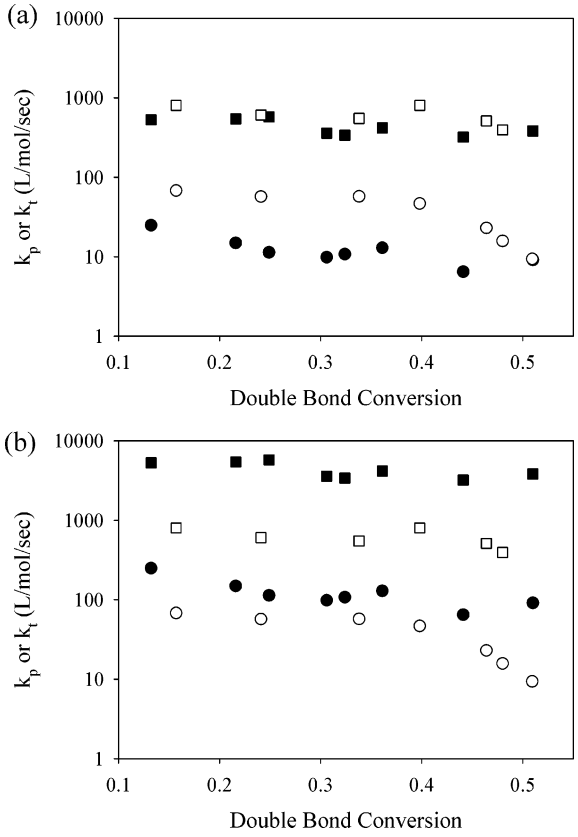

Figure 11. Apparent termination (k_t) and propagation (k_p) rate parameters of 10% HDDA initiated with 0.1 wt % DBMP in LLC phases of DTAB/water, shown as a function of double bond conversion. Given are k_t for 80% DTAB-lamellar (□), k_t for 50% DTAB-hexagonal (■), k_p for 80% DTAB-lamellar (○), and k_p for 50% DTAB-hexagonal (●). In (a) $\Phi = 0.6$ in both hexagonal and lamellar phases. Plot (b) accounts for changes in photoinitiation efficiency with $\Phi = 0.06$ in the cubic phase and $\Phi = 0.6$ in the lamellar phase.

ultimately causes an increased rate of polymerization. Clearly both monomer and photoinitiation effects vary considerably as LLC order is modulated, and both factors must be considered for a complete understanding of the complex polymerization kinetics in these ordered reaction environments.

Molecular Weight Influence. Changes in initiation efficiency not only impact polymerization kinetics but may also significantly influence the resulting polymer molecular weight when polymerizing non-cross-linking monomers. To obtain further information about the influence of LLC ordering on initiation, GPC experiments were conducted on samples polymerized using varying concentrations of surfactant and with three different initiators. *n*-Decyl acrylate was chosen for this study because it is a non-cross-linking monomer that exhibits polymerization kinetics similar to that of HDDA in the DTAB/water system.[13] Figure 12a shows the weight-average molecular weight of poly(*n*-decyl acrylate) with respect to surfactant concentration for the initiators, HEPK, DMPA, and DBMP. A significant difference in molecular weight occurs with the different initiators. Relatively high molecular weights ranging from 9×10^5 g/mol to an excess of 1×10^6 g/mol result with HEPK. Lower molecular weights result with DMPA and DBMP ranging from 7×10^5 to 8.5×10^5 g/mol. These substantial differences in molecular weight result primarily from the different UV absorbance characteristics of each initiator. HEPK has a lower extinction coefficient at 365 nm, resulting in the formation of fewer propagating radicals and longer polymer chains. DBMP and DMPA have a similar extinction coefficient at 365 nm and, as a result, yield polymers of similar molecular weight. To

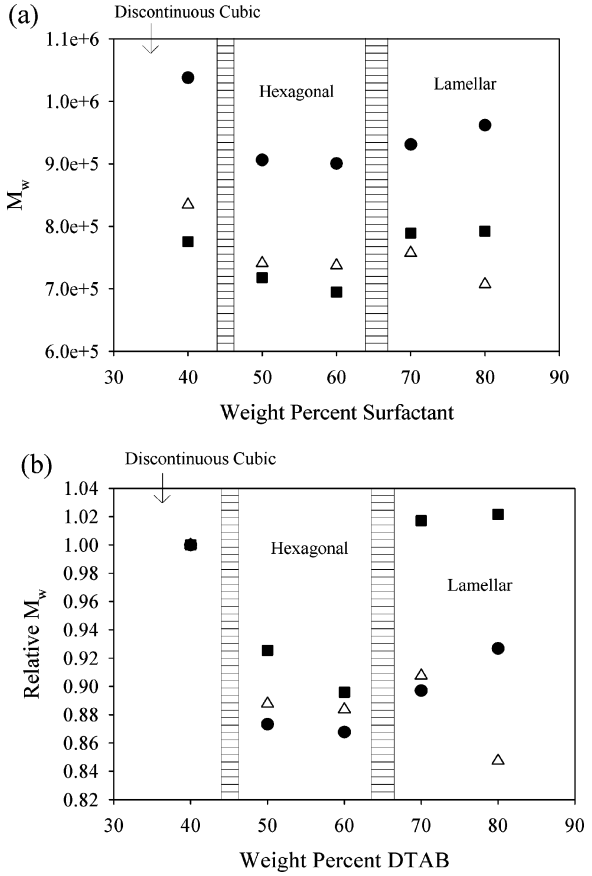

Figure 12. Absolute weight-average molecular weight (a) and relative weight-average molecular weight (b) of *n*-decyl acrylate initiated with HEPK (●), DMPA (■), and DBMP (△) as a function of surfactant concentration.

determine the effects of initiation efficiency in these systems, the trend in molecular weight for each initiator was also compared by plotting the relative weight-average molecular weight vs surfactant concentration, as shown in Figure 12b. As surfactant concentration is increased, the molecular weight initially decreases for all initiators in the study, but above 60 wt % DTAB different trends in molecular weight result with each initiator. The molecular weight from initiation with HEPK and DMPA increases between the hexagonal and lamellar phase, but with DBMP the molecular weight decreases and is lowest in the lamellar phase. Maximal double bond conversion is relatively independent of LLC phase with *n*-decyl acrylate in the DTAB/water system, and ~80% conversion is achieved with all initiators studied. Therefore, differences in monomer conversion cannot account for the distinct trends in molecular weight observed with these initiators. The decline in molecular weight at higher surfactant concentrations with DBMP can instead be explained by higher initiation efficiency, which results in a greater number of propagating radicals and a corresponding increase in polymerization rate in the more ordered reaction environment. Clearly the molecular weight evolution of polymers synthesized in LLC systems is much more complicated than that occurring in bulk. Molecular weight depends not only on the UV absorbance of the initiator but also on monomer segregation behavior and on LLC phase dependent initiation efficiency.

Conclusions

In this paper we describe a detailed analysis of the photopolymerization kinetics in lyotropic liquid crystalline media of a polar dimethacrylate and a nonpolar diacrylate monomer. By comparing the rate of polymerization in various liquid crystalline phases, the effects of monomer segregation and initiator efficiency have been elucidated. Polar and nonpolar monomers exhibit the opposite dependence of rate on LLC order as a result of their segregation in different domains within the LLC phases. By studying the effect of a free radical inhibitor on the polymerization kinetics using several common α-cleavage photoinitiators, the initiation efficiency was found to vary substantially as a function of liquid crystalline order. The efficiency depends on the size and polarity of the initiating fragments. Initiators forming large radical fragments exhibit higher efficiency in a lamellar phase relative to the cubic phase. The efficiency with smaller initiating molecules changes only slightly between these same phases because the mobility is relatively unaffected by LLC topology. The importance of initiator polarity is evidenced by the higher relative efficiency of hydrophobic initiators in phases with greater surfactant concentrations and low water content. Relatively hydrophilic initiators show the opposite dependence on surfactant concentration. The polymerization kinetics in LLC systems have been modeled by incorporating an adjustable initiation efficiency parameter to determine apparent rate parameters of propagation and termination in different LLC phases. This has led to a better understanding of the underlying causes of the interesting polymerization behavior in these highly ordered systems. As surfactant concentration is increased to induce higher degrees of ordering, initiation efficiency and monomer segregation effects may combine to cause substantial increases in the polymerization rate, or in other instances these effects may effectively cancel one another in such a way that polymerization rate changes very little with respect to LLC order.

Acknowledgment. The authors thank NSF for financial support of this project through a PECASE (CTS-0328231) grant.

References and Notes

(1) Stupp, S. I.; Pralle, M. U.; Tew, G. N.; Li, L.; Sayer, M.; Zubarev, E. R. *MRS Bull.* **2000**, *25*, 42.
(2) Paul, E. J.; Prud'Homme, R. K. In *Reactions and Synthesis in Surfactant Systems*; Texter, J., Ed.; Marcel Dekker: Rochester, NY, 2001; Vol. 100, pp 525−535.
(3) Collings, P. J.; Hird, M. *Introduction to Liquid Crystals*; Taylor & Francis Inc.: Bristol, PA, 1997.
(4) Hoag, B. P.; Gin, D. L. *Macromolecules* **2000**, *33*, 8549−8558.
(5) Pindzola, B. A.; Jin, J.; Gin, D. L. *J. Am. Chem. Soc.* **2003**, *125*, 2940−2949.
(6) Lester, C. L.; Guymon, C. A. *Polymer* **2002**, *43*, 3707−3715.
(7) Lester, C. L.; Guymon, C. A. *Macromolecules* **2000**, *33*, 5448−5454.
(8) Jin, J.; Nguyen, V.; Gu, W.; Lu, X.; Elliott, B.; Gin, D. L. *Chem. Mater.* **2005**, *17*, 224−226.
(9) Xu, Y.; Gu, W.; Gin, D. L. *J. Am. Chem. Soc.* **2003**, *126*, 1616−1617.
(10) Gin, D. L.; Gu, W. *Adv. Mater.* **2001**, *13*, 1407−1410.
(11) Sellinger, A.; Weiss, P. M.; Nguyen, A.; Lu, Y. A. R. A.; Gong, W.; Brinker, C. J. *Nature (London)* **1998**, *394*, 256.
(12) Reppy, M. A.; Gray, D. H.; Pindzola, B. A.; Smithers, J. L.; Gin, D. L. *J. Appl. Polym. Sci.* **2001**, *123*, 363−371.
(13) Lester, C. L.; Colson, C. D.; Guymon, C. A. *Macromolecules* **2001**, *34*, 4430−4438.
(14) Lester, C. L.; Smith, S. M.; Jarret, W. L.; Guymon, C. A. *Langmuir* **2003**, *19*, 9466−9472.
(15) Lester, C. L.; Smith, S. M.; Guymon, C. A. *Macromolecules* **2001**, *34*, 8587−8588.
(16) McCormick, D. T.; Stovall, K. D.; Guymon, C. A. *Macromolecules* **2003**, *36*, 6549−6558.
(17) Laversanne, R. *Macromolecules* **1992**, *25*, 489−491.
(18) Wanka, G.; Hoffmann, H.; Ulbricht, W. *Macromolecules* **1994**, *27*, 4145−4159.
(19) Holmqvist, P.; Alexandridis, P.; Lindman, B. *J. Phys. Chem. B* **1998**, *102*, 1149−1158.

(20) Holmqvist, P.; Alexandridis, P.; Lindman, B. *Langmuir* **1997**, *13*, 3, 2471−2479.
(21) Lester, C. L.; Smith, S. M.; Colson, C. D. *Chem. Mater.* **2003**, *15*, 3376−3384.
(22) Hoyle, C. E.; Chawla, C. P.; Kang, D.; Griffin, A. C. *Macromolecules* **1993**, *26*, 758−763.
(23) Hoyle, C. E.; Watanabe, T. *Macromolecules* **1994**, *27*, 3790−3796.
(24) Guymon, C. A.; Hoggan, E. N.; Clark, N. A.; Rieker, T. P.; Walba, D. M.; Bowman, C. N. *Science* **1997**, 275, 57−59.
(25) Guymon, C. A.; Bowman, C. N. *Macromolecules* **1997**, *30*, 5271−5278.
(26) Guymon, C. A.; Bowman, C. N. *Macromolecules* **1997**, *30*, 1594−1600.
(27) DePierro, M. A.; Olson, A. J.; Guymon, C. A. *Polymer* **2005**, *46*, 335−345.
(28) Encinas, M. V.; Lissi, E. A.; Rufs, A. M.; Alvarez, J. *Langmuir* **1998**, *14*, 5691−5694.
(29) Wang, L.; Liu, X.; Li, Y. *Langmuir* **1998**, *14*, 6879−6885.
(30) Kuo, P.-L.; Turro, N. J. *Macromolecules* **1987**, *20*, 1216−1221.
(31) Wang, L.; Liu, X.; Li, Y. *Macromolecules* **1998**, *31*, 3446−3453.
(32) Turro, N. J.; Cherry, W. R. *J. Am. Chem. Soc.* **1978**, *100*, 7431−7432.
(33) Turro, N. J.; Chow, M.-F.; Chung, C.-J.; Kraeutler, B. *J. Am. Chem. Soc.* **1981**, *103*, 3886−3891.
(34) Barra, M.; Bohne, C.; Zanocco, A.; Scaiano, J. C. *Langmuir* **1992**, *8*, 2390−2395.
(35) Hrovat, D. A.; Liu, J. H.; Turro, N. J.; Weiss, R. G. *J. Am. Chem. Soc.* **1984**, *106*, 7033−7037.
(36) Hrovat, D. A.; Liu, J. H.; Turro, N. J.; Weiss, R. G. *J. Am. Chem. Soc.* **1984**, *106*, 5291−5295.
(37) Kroschwitz, J.; Mark, H.; Overberger, C.; Bikules, N.; Menges, G. *Encyclopedia of Polymer Science and Engineering*; J. Wiley and Sons: New York, 1985; Vol. 1A.
(38) Kleinman, M. H.; Shevchenko, T.; Bohne, C. *Photochem. Photobiol.* **1998**, *68*, 710−718.
(39) Yarovoi, Y. K.; Shabatina, T. I.; Batyuk, V. A.; Sergeev, G. B. *Mol. Cryst. Liq. Cryst.* **1990**, *191*, 283−287.
(40) Odian, G. *Principles of Polymerization*, 4th ed.; John Wiley & Sons: New York, 2004.
(41) Kurdikar, D. L.; Peppas, N. A. *Macromolecules* **1994**, *27*, 733−738.
(42) Wen, M.; McCormick, A. V. *Macromolecules* **2000**, *33*, 9247−9254.
(43) Maliakal, A.; Weber, M.; Turro, N. J.; Green, M. M.; Yang, S. Y.; Pearsall, S.; Lee, M.-J. *Macromolecules* **2002**, *35*, 9151−9155.
(44) Russell, G. T.; Napper, D. H.; Gilbert, R. G. *Macromolecules* **1988**, *21*, 2141−2148.
(45) Rubingh, D. N.; Holland, P. M. In *Cationic Surfactants: Physical Chemistry*; Holland, P. M., Ed.; Marcel Dekker: New York, 1991; Vol. 37.

MA0518196